Chapter

# Soliton Like-Breather Induced by Modulational Instability in a Generalized Nonlinear Schrödinger Equation

*Saïdou Abdoulkary and Alidou Mohamadou*

## Abstract

We consider the nonlinear Schrödinger equation modified by a rational nonlinear term. The model appears in various studies often in the context of the Ginzburg-Landau equation. We investigate modulational instability by means of a linear stability analysis and show how the nonlinear terms affect the growth rate. This analytical result is confirmed by a numerical simulation. The latter analysis shows that breather-like solitons are generated from the instability, and the effects of the nonlinear terms are again clearly seen. Moreover, by employing an auxiliary-equation method we obtain kink and anti-kink soliton as analytical solutions. Our theoretical solution is in good agreement with our numerical investigation.

**Keywords:** generalized nonlinear schrödinger, modulational instability, breather like-soliton

## 1. Introduction

The nonlinear Schrödinger equation (NLSE) is the main equation which governs the propagation of pulses in various fields such as nonlinear optical systems, plasmas, fluid dynamics, Bose-Einstein condensation, and condensed matter physics. It has been shown to govern the evolution of a wave packets in weakly nonlinear and dispersive media and has thus arisen in such diverse fields. One other application of this equation is in pattern formation, where it has been used to model some nonequilibrium pattern forming systems. Most notable is the role it plays in understanding the propagation of electromagnetic waves in glass fibers and other optical waveguides [1].

In this paper we consider a NLS equation with inverse nonlinear terms. Inverse nonlinear term has been introduced for the first time by Malomed and al. [2] which has been later studied by [3, 4] in the case of the Ginzburg-Landau equation.

$$iu_z + pu_{xx} + \gamma_1 \frac{\left|\frac{\partial u}{\partial x}\right|^2}{|u|^2} u + \gamma_2 \frac{1}{|u|^2} u + \gamma_3 |u|^2 u = 0, \tag{1}$$

where $u$ is a complex amplitude that depends on $z$ and $x$, $\gamma_i$ $(i = 1, 2, 3)$ is a real constant and represents the nonlinear coefficient, $p$ is a real constant and supposes

to be the group-velocity dispersion (GVD) coefficient. Notice that Eq. (1) especially with $\gamma_1 = \gamma_2 = 0$ appears in many contemporary work in physics and has been shown to be completely integrable [5] and to admit optical solitons by balancing the GVD and Kerr nonlinearity $\gamma_3$ (the self-focusing interaction and defocusing interaction corresponding to bright and dark solitons, respectively). However, in many applications it contains also some small additional terms which destroy these properties. It describes either the propagation of a continuous wave (CW) beam in a planar waveguide or propagation of an optical pulse inside optical fiber, and show that this equation admits analytical solitary solution and exhibits a modulation instability (MI). This instability leads to spatial or temporal modulation of a constant-intensity plane wave.

Modulational instability is one of the nonlinear wave equations associated to NLSE and appears in many physical systems. It indicates that due to the competition between nonlinearity and the dispersive effects, a small perturbation of the initial plane wave may induce an exponential growth of the wave amplitude, resulting in the carrier-wave breakup into a train of localized waves [6].

The NLSE is also one of the original nonlinear partial differential equations, the study of which has lead to fundamental advances in theoretical physics. The study of NLS was motivated by a large number of theoretical problems ranging from optical pulse propagation in nonlinear fibers to hydrodynamics, condensed matter physics and biophysics. It is now known that NLS is one of the few examples of completely integrable nonlinear partial differential equations [7, 8].

The main objective of this paper is to study MI in a generalized NLSE that includes rational nonlinear terms given by Eq. (1). By means of the linear stability analysis we explicitly investigate the stability condition of a launched plane wave. The results show that the MI gain is strongly dependent on the nonlinear parameters as well as the GVD. Our numerical simulations show that those parameters contribute to the formation and the propagation of the soliton like-breather in the systems. Those parameters can generate either stable or unstable solitons. We also investigate analytical soliton solutions. By employing auxiliary equation method we obtain kink and antikink solutions of Eq. (1).

The rest of the paper is organized as follows. The model is introduced in Section 2, which is followed by the analysis of the MI of the CW solutions in Section 3, direct simulations shown the formation of modulated wave as well as breather like-solitons and their stability in Section 4. Exact analytical kink and antikink soliton solutions are reported in Section 5, and the paper is concluded by Section 6.

## 2. Modulational instability

The nonlinear Schrodinger Equation Eq. (1) has the simplest solution in the form of a continuous wave as $u = u_0 \exp i(kx - \omega z)$, where $u_0$ is a constant and $k$ and $\omega$ are respectively the the wave-number and the angular frequency and satisfy the dispersion relation $\omega - k^2 p + \gamma_1 k^2 + \frac{\gamma_2}{|u_0|^2} + \gamma_3 |u_0|^2 = 0$. Now we focus our attention on the modulational instability in the system. Therefore, we look at solutions of Eq. (1) in the form of

$$u = u_0(1 + b) \exp i(kx - \omega z), \tag{2}$$

where $b$ represents a small perturbation.

Substituting Eq. (2) into the NLS equation Eq. (1) and linearizing the resulting equations, we obtain a linear equation of $b$.

$$ib_z + pb_{xx} + 2ikpb_x + i\gamma_1 k\left(b_x^* - b_x\right) - \frac{\gamma_2}{|u_0|^2}(b^* + b) + \gamma_3|u_0|^2(b^* + b) = 0, \quad (3)$$

Looking for solutions to this function in the form of plane waves $b = b_1 \exp i(Kx - \Omega z) + b_2^* \exp -i(Kx - \Omega z)$, we obtain the dispersion relation

$$\Omega = (2p - \gamma_1)kK \pm K\sqrt{\gamma_1^2k^2 + p^2K^2 + 2\frac{\gamma_2}{|u_0|^2}p - 2\gamma_3 p|u_0|^2}, \quad (4)$$

where the wave number $K$ and the frequency $\Omega$ characterize linear properties of the modulation wave. The dispersion relation given by Eq. (4) determine the condition for the stability of a plane wave with a wave number $k$ in the system. This is the case as long as $\Omega$ is real. This stability condition is explicitly depends on the nonlinear parameters $\gamma_1$, $\gamma_2$, and $\gamma_3$. It shows that the CW plane-wave is absolutely stable only in the case $\gamma_1^2k^2 + p^2K^2 + 2\frac{\gamma_2}{|u_0|^2}p - 2\gamma_3 p|u_0|^2 < 0$. That is

$$\left(\gamma_1^2k^2 + p^2K^2\right) - \sqrt{\Delta} < |u_0|^2 < \left(\gamma_1^2k^2 + p^2K^2\right) + \sqrt{\Delta}, \quad (5)$$

with $\Delta = \left(\gamma_1^2k^2 + p^2K^2\right)^2 + 16\gamma_2\gamma_3p^2$.

The modulation instability gain is related to the imaginary part of $\Omega$ and is given by

$$g = Im\left[|K|\sqrt{\gamma_1^2k^2 + p^2K^2 + 2\frac{\gamma_2}{|u_0|^2}p - 2\gamma_3 p|u_0|^2}\right], \quad (6)$$

**Figure 1** shows the instability gain as a function of the perturbation wave number $K$ for $u_0 = 1$ and 1.5. The gain exists for both positive and negative values of $K$ in the range $|K| < K_0 = (1/2)\sqrt{-2\gamma_1^2k^2|u_0|^2 - 4\gamma_2 p + 4\gamma_3 p|u_0|^4}/(|u_0|p)$. The peak gain occurs for $K = K_0$ and has the value $g_{max} = (1/2)K_0|\sqrt{2\gamma_1^2k^2 + 4\gamma_2 p/|u_0|^2 - 4\gamma_3 p|u_0|^2}|$. Now let us study the latter gain. We have plotted a qualitative study of its behavior. **Figure 1a** shows that the peak gain increased with the amplitude $u_0$ increasing as well as it width. In **Figure 1b** one can see the inverse phenomenon. **Figure 2** shows the evolution of the peak gain as a function of nonlinear parameters $\gamma_2$ and $\gamma_3$. Here we are seeing the

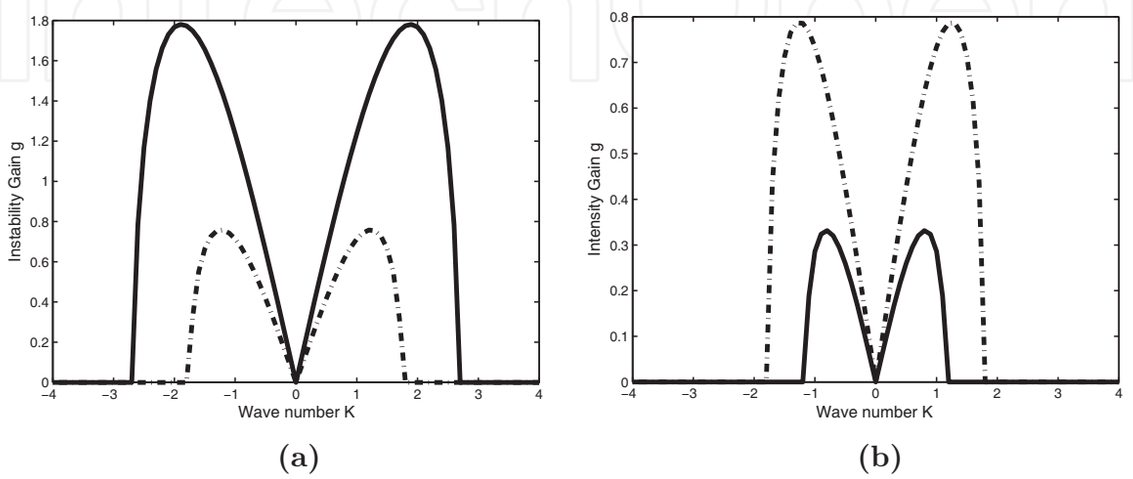


**Figure 1.**
*Gain spectrum $g(K)$ of modulation instability as a function of wave number with effect of the background amplitude $u_0 = 1$ (dashed line) and 1.5 (soline) when the GVD is 0.5 for the left-hand panel (a) with $\gamma_1 = 0.1$, $\gamma_2 = 0.4$, $\gamma = 0.8$ and the GVD is $-0.5$ for the right hand-panel (b) with $\gamma_2 = 0.8$, $\gamma_3 = 0.01$.*

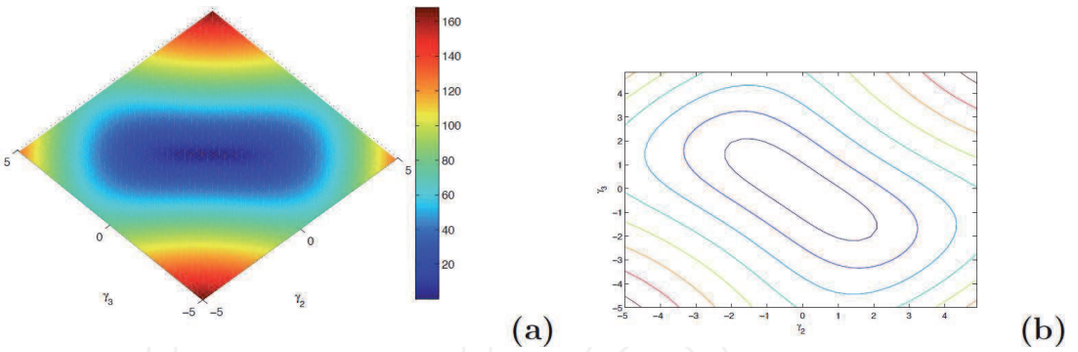


**Figure 2.**
*Maximum gain spectrum $g_{max}$ of modulation instability for $u_o = 1$ versus nonlinear parameters $\gamma_2$ and $\gamma_3$ (panel (a)), while in panel (b) we show its contour plot.*

increasing of the peak with the nonlinear terms (see **Figure 2a**). There is a limit cycle where the peak remains constant for certain values of both $\gamma_2$ and $\gamma_3$. This is clearly seen through the contour plot in **Figure 2b**. This aspect is better analyzed in **Figure 3** where the peak gain increased by increasing both $\gamma_2$ and $\gamma_3$ in the left side of top panel (a) as well as the gain width. This is confirm by fixing one nonlinear parameter ($\gamma_2$)

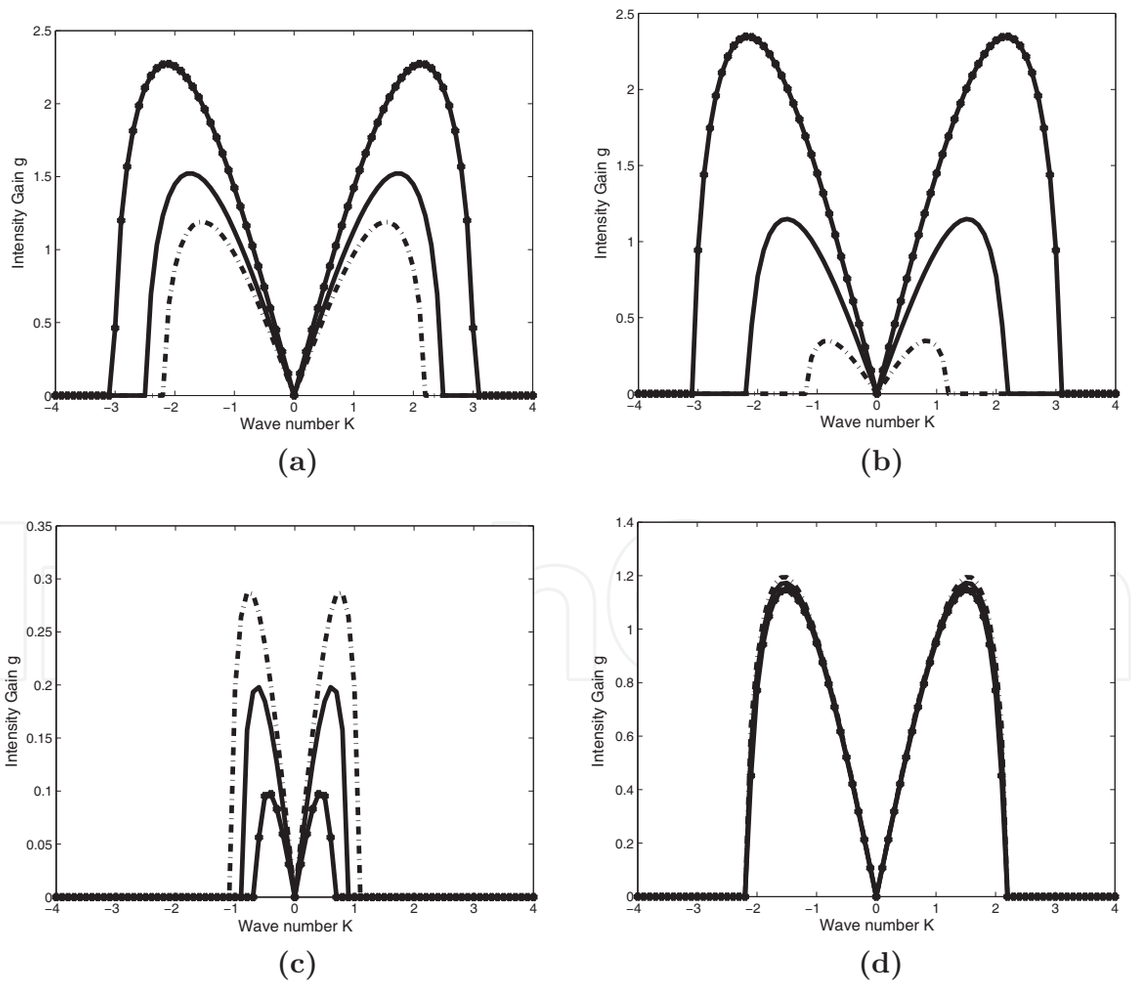


**Figure 3.**
*Gain spectrum $g(K)$ of modulation instability as a function of wave number with effect of the nonlnear parameters $\gamma_2$, $\gamma_3$. In the top panel (a) on left we set $\gamma_2 = 0.03$, $\gamma_3 = 0.3$ for dashed line, $\gamma_2 = 0.3$, $\gamma_3 = 0.4$ for the solid line, $\gamma_2 = 0.5$, $\gamma_3 = 0.6$ for o-line. On right (b) we set $\gamma_2 = 0.2$, and $\gamma_3 = 0.1, 0.3, 0.6$ (respectively for dashed, solid and o-line. In botton we got on left panel (c) $\gamma_2 = 0.01, 0.1, 0.2$ (respectively for dashed, solid and o-line) and $\gamma_3 = 0.3$. For all the previous panels we got $u_o = 1$ and $\gamma_1 = 0.1$. On right panel (d) we consider the same values in (c) when $u_o = 2$.*

when the last one ($\gamma_3$) is varying (see panel (b)). One observe the inverse phenomenon by fixing $\gamma_3$ when $\gamma_2$ increasing (see panel (c)). The last panel (d) is very particular while we are seeing the peak and the width gain are almost constant by varying the nonlinear parameters ($\gamma_2$) when the background amplitude $u_0 = 2$.

## 3. The numerical simulation analysis

Analytical analysis done by linear stability shown the possibility of the formation of modulated waves in the consider system. This prediction can be numerically confirmed. In this way let us launch as initial condition a modulated plane wave: $u(0,x) = 1 + \varepsilon \cos(Kx)$ where fixed boundary conditions are used and the numerical constants used in the calculation are the following: $\varepsilon = 0.01$, $p = 0.5$, $k = 0$, $K = 0.2\pi$, $\gamma_1 = 0.1, 0.2, 0.3$ in $\gamma_2 = 0.01, 0.1, 0.4, 0.6$ and $\gamma_3 = 0.1, 0.3, 0.6, 0.9$ normalized units. The question we are going to answer is the influence of the parameters $\gamma_i$ on the formation of modulated wave.

From **Figure 4** one can see the formation of bright solitary wave. The left hand top panel shows the generation of a pulse train toward the boundary regions but the intensity is smallest at the center. On right hand panel we can see the bright solitary wave behaves like a breather soliton is forming. This may be a multisoliton quasiperiodic solutions. It can be seen that the breather solutions keep their oscillating shapes, while the wave packets move as periodic solitons along the $x$-axis for certain values of $z$. Those breathers are periodic in the $x$ coordinate and aperiodic in the $z$ coordinate. There is more generation of breathers in bottom panels (e) and (f). Comparing panel (b) with panels (e) and (f), one can see that in panels (e) and (f), under the influence of the increasing values of the parameter $\gamma_3$, the number of peaks on the same space interval is increasing when $|x|$ goes up even $z$. The breathers have compressed in width and peak, and this is clearly seen through the contour plot figures given by panels (c), (d), (g) and (h). Those phenomenon are certainly caused by increasing of the nonlinear parameter $\gamma_3$ when $\gamma_2$ remains small and constant. We can see the evolution of the peak amplitude of the wave over the z-axis for each case above in **Figure 5**. One can see that in panel (a) the peak amplitude increases gradually and oscillation little beat over the parameter $z$. The oscillation of the peak is increasing when the nonlinear parameter $\gamma_3$ increases and the curve believes sharp. This is perceptible in the rest panels (b, c and d). One can clearly confirms The dynamical process of the spatial pattern formation induced by MI. When $\gamma_3$ increases, the rate of MI increases too and the MI occurs earlier. Another interesting phenomenon is the width of the breather which decreases by increasing the consider nonlinear parameter.

There is more breathers when $\gamma_2$ is negative. **Figure 6** shows the evolution of the typical intensity profile done by numerical simulations. In panel (a) one can see that there are more breathers that appears more stable than the previous one. This analysis is more perceptible in panel (b) where we plot the contour plot of the consider figure. We are seeing both presence of breathers and bright soliton. This means that the consider parameter is strongly responsible of the formation of those solitons. This is more view in **Figure 7** where panels (a) and (b) shown how breathers are broke and the bright soliton takes place and propagate through the system when the wave vector is small than the previous one ($0.01\pi$).

## 4. Exact analytical solutions to the consider stationary model

We now discuss about the analytical solution to the stationary NLS of Eq. (1). Suppose that

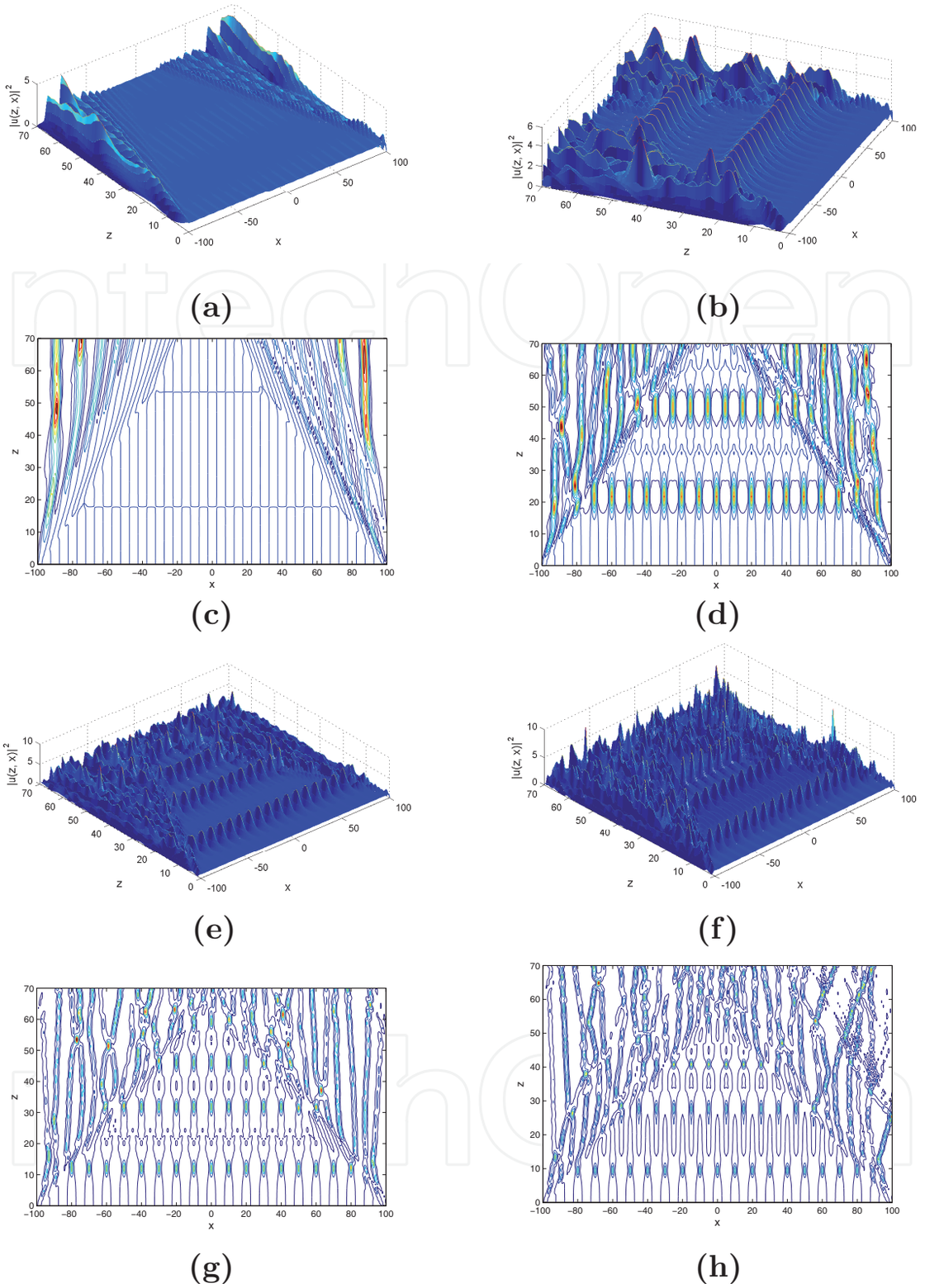


**Figure 4.**
*The evolution of the typical intensity profile done by numerical simulation of Eq. (1) when $\gamma_3$ is varying (0.1, for (a), 0.3 for (b), 0.6 for (e) and 0.8 for (f)) by fixing $\gamma_1 = 0.1$ and $\gamma_2 = 0.01$, while panels (c), (d), (g) and (h) show their respective contour plots.*

$$u(z,x) = V(x)\, exp\,[i\phi(z)], \tag{7}$$

is the solution of Eq. (1) where $V$ is independent of $z$ and $\phi$ the phase. Substituting Eq. (7) into Eq. (1) we obtain two equations for $V$ and $\phi$. The phase equation shows that $\phi$ should be of the form $\phi(z) = \beta z$, where $\beta$ is a constant and $V$ equation is

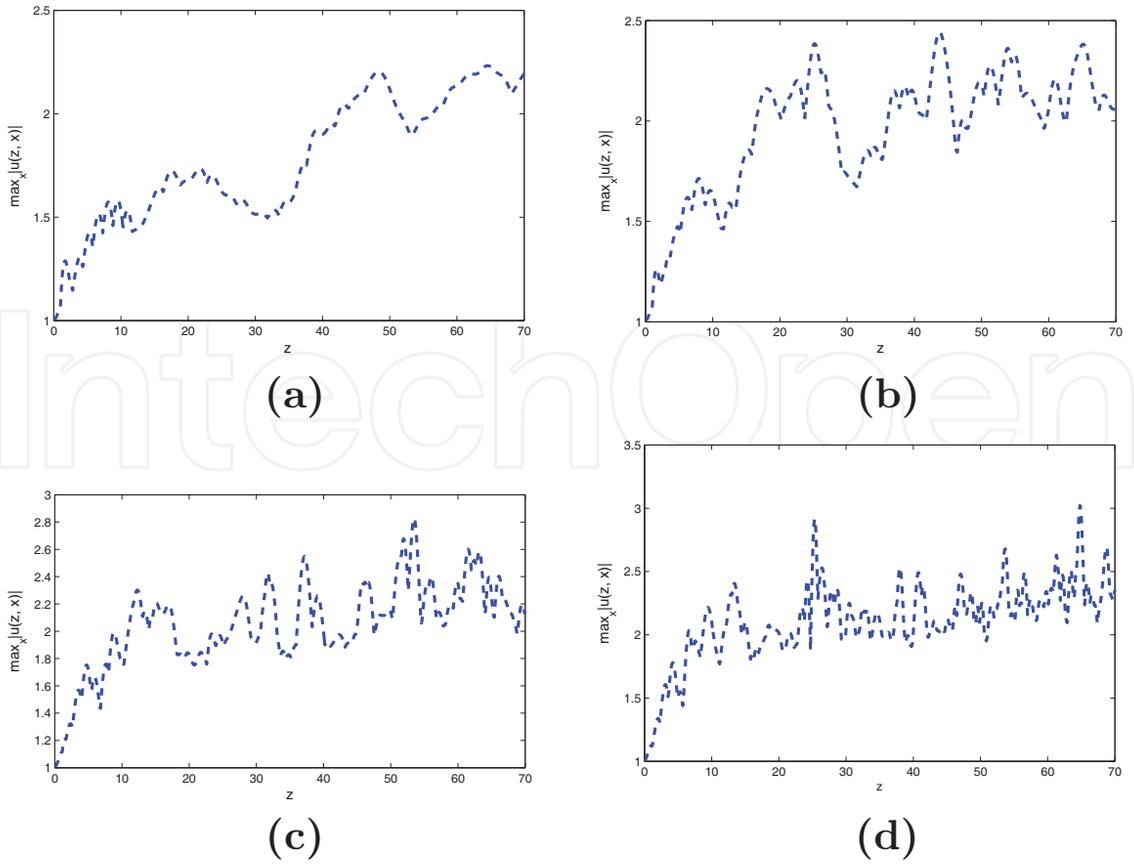


**Figure 5.**
*Representation of the maximum amplitude versus z corresponding of each panels (a), (b), (e) and (f) of* ***Figure 4*** *respectivelly.*

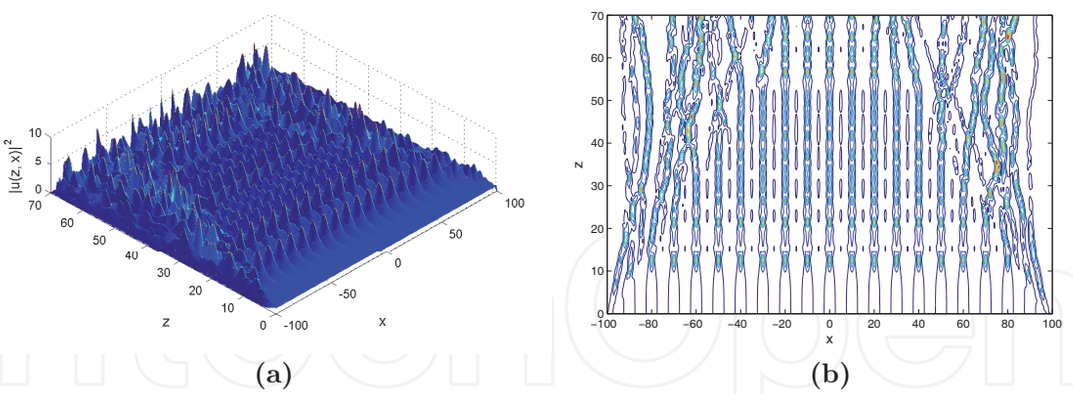


**Figure 6.**
*The influence of negative value of $\gamma_2$ on the evolution of the typical intensity profile done by numerical simulation of Eq. (1) with $p = 1/2$, $\gamma_1 = 0.1$, $\gamma_2 = -0.2$, $\gamma_3 = 0.4$ showed by panel (a), while panel (b) shows its contour plot.*

$$-\beta V + pV_{xx} + \gamma_1 \frac{V_x^2}{V} + \gamma_2 \frac{1}{V} + \gamma_3 V^3 = 0, \tag{8}$$

For solving this equation we set $V = G^{\frac{1}{2}}$ and then the Eq. (8) yields

$$\frac{1}{4}(\gamma_1 - p)\dot{G}^2 + \frac{1}{2}pG\ddot{G} + \gamma_2 G - \beta G^2 + \gamma_3 G^3 = 0, \tag{9}$$

This is a nonlinear ordinary differential equation which can be solve by the auxiliary equation method.

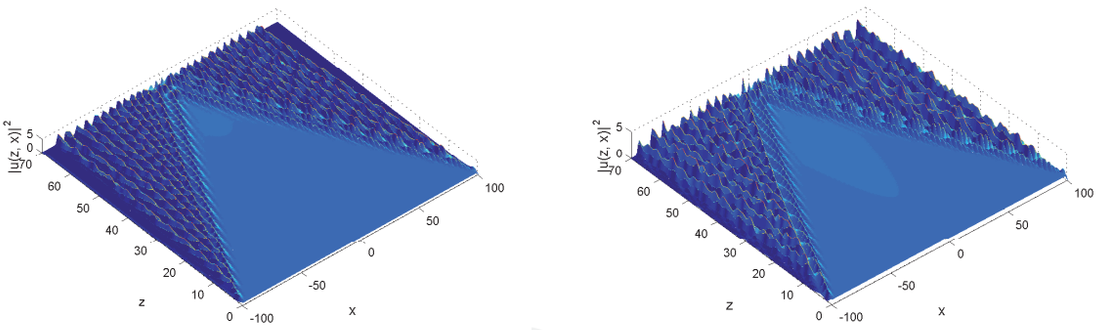


**Figure 7.**
*Influence of $\gamma_2$ and wave number K on the evolution of the typical intensity profile done by numerical simulation of Eq. (1) when $\gamma_2 = -0.03$ in (a) and $\gamma_2 = 0.03$ (b), the rest of the parameters are $\gamma_1 = 0.1$, $\gamma_3 = 0.5$ and $K = 0.01\pi$.*

### 4.1 The auxiliary equation method

The auxiliary equation method has been defined by [9, 10] while it allows to find more and new multiple solutions for nonlinear partial differential equations. The main steps of using this method is summarized as follows.

For solving equation

$$P(u, u_t, u_x, u_{xx}, u_{xxx}, \ldots) = 0, \tag{10}$$

we set $\xi = x + \omega t$ then the nonlinear partial differential equation in two independent variables $(x, t)$ becomes a nonlinear ordinary differential equation

$$Q\left(u, u', u'', u''', \ldots\right) = 0, \tag{11}$$

We seek for the solutions of Eq. (11) in the following generalized form

$$u(\xi) = \sum_{i=0}^{2M} a_i F^i(\xi), \tag{12}$$

in which $a_i$ (i = 0, 1, 2, … , 2 M) are constants to be determined and $M = 2$. The variable $F(\xi)$ should satisfy the following variable separated ordinary differential equation

$$F'^2(\xi) = aF^2(\xi) + bF^4(\xi) + cF^6(\xi), \tag{13}$$

where $a, b, c$ are parameters to be determined. Substituting Eq. (12) into (11) by taking in account Eq. (13) and equate the coefficients of all powers of $F(\xi)$ to zero yields a set of algebraic equations for unknowns $a, b, c, a_i$ (i = 0, 1, … , 2 M) and $\omega$. We solve the set of algebraic equations by the use of Maple and substitute the solutions obtained in this step back into (12) so as to obtain the exact traveling wave solutions for Eq. (10).

The solution of Eq. (9), balancing $GG''$ with $G^3$ gives $M = 2$. Therefore we may choose

$$G'^2 = a_0 + a_1 F(\xi) + a_2 F^2(\xi) + a_3 F^3 + a_4 F^4, \tag{14}$$

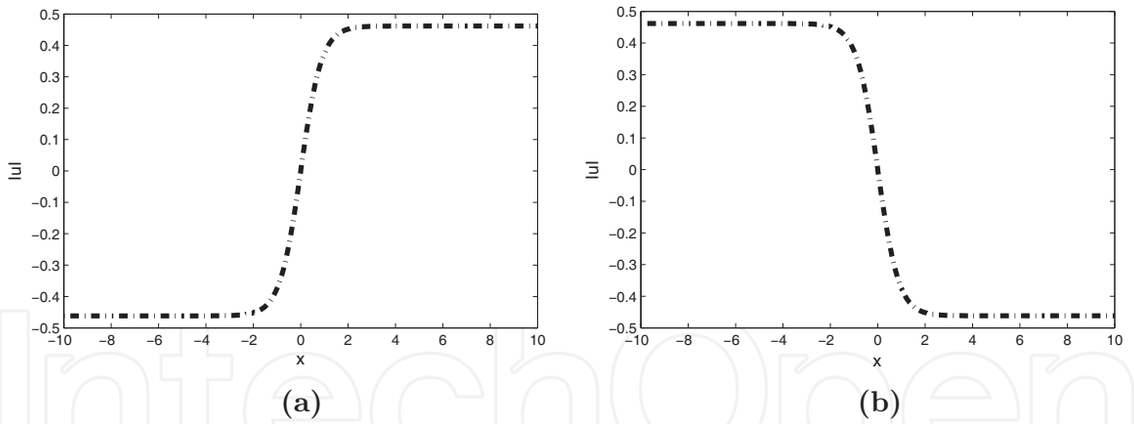


**Figure 8.**
*Kink and anti-kink representations of the analytical solutions done by Eq. (16). The following parameter values are used* $p = 1/2$, $\gamma_1 = -1.1$, $\gamma_2 = 0.3$ *and* $\gamma_3 = 0.6$.

where $a_0$, $a_1$ and $a_2$, $a_3$, $a_4$ are constants to be determined. By applying the defined method we obtained the following exact kink and anti-kink solutions for the stationary NLSE (9).

$$G = \pm\sqrt{a_0}\tanh\left(x\sqrt{a}\right), \tag{15}$$

where $a_0 = \sqrt{\frac{\gamma_2}{\gamma_3}\left(1+\frac{2p}{\gamma_1}\right)}$ and $a = -\frac{\gamma_2}{\gamma_1 a_0}$. We must have $\gamma_2/\gamma_1 < 0$ in order to ensure that the pulse width $\sqrt{a}$ is real.

Having obtained exact solutions of the stationary NLSE Eq. (9), we will use them together to construct soliton solutions of the NLSE Eq. (1). In this case, the kink-soliton and anti-kink solutions of Eq. (1) can be written in the form

$$u(z,x) = \pm\sqrt{a_0}\tanh\left(x\sqrt{a}\right)\exp i\beta z, \tag{16}$$

where $\beta = 2a(\gamma_1 + p)$. **Figure 8** shows the representation of the analytical solution to the stationary NLSE.

## 5. Conclusion

In the present study a generalized nonlinear Schrödinger equation with particular nonlinearities has been introduced. The model including rational nonlinearity that arise from Malomed model and describes the propagation of nonlinear surface waves on a plasma with a sharp boundary. We explicitly investigated MI gain by means of linear stability analysis. Results reveal that the nonlinear parameters are strongly influences the dynamics of the launched plane wave. We further tested the evolutionary modulate plan wave numerically, which indicates that those parameters allow the formation of breather-like soliton in the system as well as bright soliton. We have investigated analytical kink and anti-kink soliton too.

It would be particularly worthwhile to extend this study to the generalized NLS with time and space modulated nonlinearities and potentials. This could allow more stability and more formation of the breather-like soliton as well as the Akhmediev breather [11], Peregrine rogue wave [12], and Kuznetsov-Ma breather [13, 14] and even high-order rogue waves [15]. MI gain distributions could bring different nonlinear excitation pattern dynamics.

## Classification

PACS numbers: 05.45,Yv, 04.20.Jb, 42.65.Tg



## Author details

Saïdou Abdoulkary[1*] and Alidou Mohamadou[2,3]

1 Département des Sciences Fondamentales, FMIP, University of Maroua, Maroua, Cameroon

2 National Advanced School of Engineering of Maroua, Maroua, Cameroon

3 The Abdus Salam International Centre for Theoretical Physics, Trieste, Italy

*Address all correspondence to: elsaidais@yahoo.fr

## References

[1] G. P. Agrawal, *Nonlinear Fiber Optics* (Academic, California, 2001).

[2] B. A. Malomed, L. Stenflo, J Phys A: Math Gen **24** L1149 (1991).

[3] E. Yomba, T. C. Kofane, Chaos, Solitons and Fractals **17** 847 (2003).

[4] A. Mohamadou et al. Chaos, Solitons and Fractals **27** 914–925 (2006).

[5] V. E. Zakharov and A. B. Shabat, Zh. Eksp. Teor. Fiz. **61**, 118 (1971) [Soy. Phys. JETP 34, 62 (1972)].

[6] L.Q. English, M. Sato, A.J. Sievers, Phys. Rev. B **67**, 024403 (2003).

[7] D. Hennig, G. P. Tsironis, Physics Reports **307** (1999) 333-432.

[8] M. J. Ablowitz, P. A. Clarkson, *Solitons, Nonlinear Evolution Equations and Inverse Scattering*, Cambridge Univ. Press, New York, 1991.

[9] Sirendareji, Phys. Lett. A **356** (2006) 124.

[10] S. Abdoulkary et al., Appl. Math. Comput. **233** (2014) 109-115.

[11] N. Akhmediev and V. I. Korneev, Theor. Math. Phys. **69**, 1089 (1986).

[12] D. H. Peregrine, J. Aust. Math. Soc. Ser. B 25, **16** (1983).

[13] E. A. Kuznetsov, Sov. Phys. Dokl. **22**,507(1977).

[14] Y. C. Ma, Stud. Appl. Math. **60**, **43** (1979).

[15] B. L. Guo, L. M. Ling, and Q. P. Liu, Phys. Rev. E **85**, 026607 (2012).